Chapter 6
Effects of Biodiesel Usage on Fuel Spray Characteristics

The spatial and temporal distribution of a fuel spray in a diesel engine has a determining effect on noise and exhaust emissions, fuel consumption, and engine performance (Battistoni and Grimaldi 2012; Kuti et al. 2013; Park et al. 2008). The most important fuel spray characteristics are *spray penetration*, *spray angle*, and *Sauter mean diameter*. These characteristics depend to a great extent on the injector type, fuel composition, and engine operating regime (Kousoulidou et al. 2012; Lin and Lin 2011; Mancauruso et al. 2011).

Spray development depends significantly on the processes occurring within the injector orifice, turbulence and cavitation being perhaps the most important. Once the fuel exits the orifice, spray development is determined by the fuel atomization process. Unfortunately, all the mechanisms acting in this phase are still not fully understood. Because various mechanisms are in action and because the magnitude of their influence may depend significantly on several circumstances, it is very difficult to make concise and unique conclusions. In other words, what is observed under some circumstances may change substantially under somewhat modified situation.

The *injector type influence* is largely determined by its control and geometric parameters. Among the control parameters, the injection pressure is probably the most important; its influence will be addressed along with the effects of engine operating regime. On the other side, the most important geometric parameters are those related to the injector nozzle geometry. Roughly speaking, there are two main orifice geometries: the more common cylindrical and the conical orifice. A major difference between these two types is the presence of cavitation phenomena, which is much more exposed in the cylindrical orifice. The most important parameters of the nozzle are related to the (one or more) *orifice diameters*, its *length*, and the *shape* of the *orifice inlet* (sharp or rounded edges).

In general, smaller orifice diameters (combined with higher injection pressures) lead to better atomization and surface evaporation of the spray. For example, several investigations show that the usage of high injection pressure and a micro-hole nozzle represents an effective method to improve spray atomization and mixture preparation processes of biodiesel fuels (Kuti et al. 2013). On the other

B. Kegl et al., *Green Diesel Engines*, Lecture Notes in Energy 12,
DOI 10.1007/978-1-4471-5325-2_6, © Springer-Verlag London 2013

side, the shape and dimension of the nozzle hole have a notable influence on the cavitation phenomena, fuel exit velocity, and the discharge coefficient. In general, an increase of the orifice inlet radius leads to increased mean exit velocity and discharge coefficient near the orifice wall, while the region of the cavitation contracts.

Since fuel composition has also an important influence on spray characteristics, one can expect that a replacement of mineral diesel by biodiesel will also have significant effects. In fact, biodiesel usage usually results in longer spray tip penetration and narrower cone angles; this is mostly attributed to poorer atomization characteristics of biodiesels. Furthermore, compared to mineral diesel, the liquid lengths of biodiesels are higher due to higher boiling temperature and vaporization heat of biodiesel fuels.

Fuel spray development, especially in its early phase, depends heavily on the injection rate and spray momentum, which is the energy of the spray, delivered at the nozzle exit (Desantes et al. 2009). These quantities vary in dependence on the engine operating regime. This means that spray development has to be investigated at various engine loads and speeds.

6.1 Spray Penetration

Spray tip penetration is most significantly affected by the fuel *density*, *viscosity*, and *surface tension* (Kegl 2008; Pogorevc et al. 2008; Yoon et al. 2009). This influence varies in dependence on the engine operating regime.

6.1.1 Influence of Biodiesel Properties

In general, biodiesels have higher density, viscosity, surface tension, and bulk modulus than mineral diesel. Higher density increases the momentum of the injected fuel. Furthermore, in mechanically controlled fuel injection systems, higher density and higher bulk modulus also mean higher injection pressures. This means that, in general, higher density and bulk modulus will result in higher penetration lengths. Higher viscosity and surface tension result in poorer fuel vaporization. This is another reason for higher penetration lengths. On the other hand, higher viscosity means higher friction between the fuel and the injector nozzle surface. Under some circumstances this may result in lower penetration lengths, for example, in the case of some biodiesel blends with mineral diesel.

Obviously, one can expect that biodiesel usage will prolong the penetration lengths. This may lead to serious problems, if the liquid part of the spray reaches the combustion chamber wall and the piston surface. Heavy carbon deposits on the walls, piston ring sticking and breaking, and dilution of the lubricating oil may be the consequences (Pandey et al. 2012).

Table 6.1 Investigation data (Kuti et al. 2013)

Injection system/injector	Common rail for DI diesel engine
Nozzle type	Single hole
Length of nozzle hole	1.2 mm
Nozzle hole diameter	0.08 mm and 0.16 mm
Injection pressure	2,000 bar
Injection duration	1.5 ms
Ambient temperature	885 K
Ambient pressure	40 bar

In the following, the effects of variable fuel properties on fuel spray tip penetration are discussed by using several types of biodiesel in various injectors of mechanically and electronically controlled fuel injection systems.

In Kuti et al. (2013) spray tip penetration of *palm biodiesel* (PaBIO) was investigated numerically and experimentally in a diesel engine with a *common rail injection system* (Table 6.1). The experimental conditions were similar to real engine conditions. The constant volume vessel was filled with nitrogen gas.

The results revealed that a change from mineral diesel (D100) to PaBIO results in longer spray tip penetration at both tested nozzle hole diameters (Fig. 6.1). Furthermore, it was evident that the spray tip penetration is higher for the nozzle hole with larger diameter. This is true for both fuels, D100 and PaBIO. It was observed that after an initial spray development period, the tip of the liquid phase fuel region stopped penetrating and fluctuated about a mean axial location as a result of turbulence. The PaBIO produced longer liquid phase lengths than D100. This implies that D100 evaporated more quickly than PaBIO. One reason for that is obviously the higher boiling point of PaBIO, which is characterized by the distillation temperature. Because of the high boiling point property, PaBIO is less volatile than D100. As a result of less volatility, PaBIO produces longer liquid phase lengths and the energy required to heat and vaporize PaBIO is higher. Since the entrainment rate of energy into the spray is limiting the vaporization process, the requirement for more energy to heat and vaporize the less volatile fuel translates to a longer spray tip penetration.

In Battistoni and Grimaldi (2012) an extensive experimental and numerical research of the influence of various *nozzle hole types* on D100 and *soybean biodiesel* (SoBIO) spray penetration has been done. The numerical part was based on 3D simulation of the unsteady multiphase flow in the injector (Table 6.2).

The results show that higher flow rates were achieved by the conical nozzle. This is because cavitation phenomena in a conical orifice are far less exposed than in a cylindrical orifice. Consequently, the penetration lengths obtained with the conical orifice are notably higher than those obtained with the cylindrical orifice. This can be observed for both fuels, D100 and SoBIO. What is quite interesting here is that the penetration length differences are much larger for D100 than for SoBIO. Figure 6.2 shows the relative variations of the penetration lengths when the cylindrical orifice is replaced by a conical one. Although for SoBIO the conical

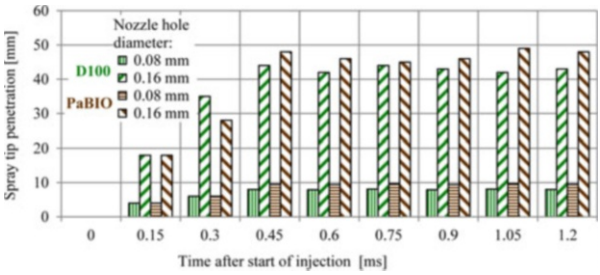

Fig. 6.1 Influence of nozzle hole diameter on fuel spray penetration

Table 6.2 Investigation data (Battistoni and Grimaldi 2012)

Injection system/injector	Common rail Bosch CRI1
Nozzle type	Mini-sac, five holes: cylindrical and conical orifice shape
Length of nozzle hole	0.7 mm
Nozzle hole diameter	0.13 mm
Injection pressure	1,350 bar
Energizing duration	0.5 ms
Ambient pressure	10 bar

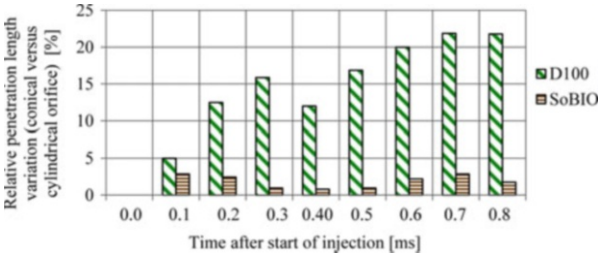

Fig. 6.2 Influence of nozzle hole type on fuel spray penetration

shape results in a slightly higher penetration length, the relative length variation with respect to the length, obtained with the cylindrical orifice, is rather minor.

In Kegl (2008) and Pogorevc et al. (2008) fuel spray penetration of *rapeseed biodiesel* (RaBIO) in a bus diesel engine with a mechanically controlled M injection system (Table 6.3) was investigated numerically and experimentally. The fuel was injected through a one-hole nozzle into a glass chamber at room temperature and atmospheric pressure and filmed with a high-speed digital camera.

The fuel spray development for D100 and RaBIO at partial load of 50 % and 500 rpm is shown in Fig. 6.3. It is evident that RaBIO spray is longer than that of mineral diesel by about 5 %. Partially, this is because RaBIO atomizes poorly compared to mineral diesel due to its higher surface tension, density, and viscosity. On the other hand, RaBIO usage results in a stepper rise and higher injection pressure, which also influences the development of the spray.

In Wang et al. (2010, 2011) the liquid lengths of PaBIO and *waste cooking biodiesel* (WcBIO) were investigated under simulated diesel engine conditions in a constant volume chamber (Table 6.4). A common rail injection system was used to

Table 6.3 Investigation data (Kegl 2008)

Injection system/injector	Direct injection system with wall distribution (M system)
Nozzle type	Single hole
Length of nozzle hole	1.95 mm
Nozzle hole diameter	0.68 mm
Needle opening pressure	175 bar
Needle lift (maximum)	0.3 mm

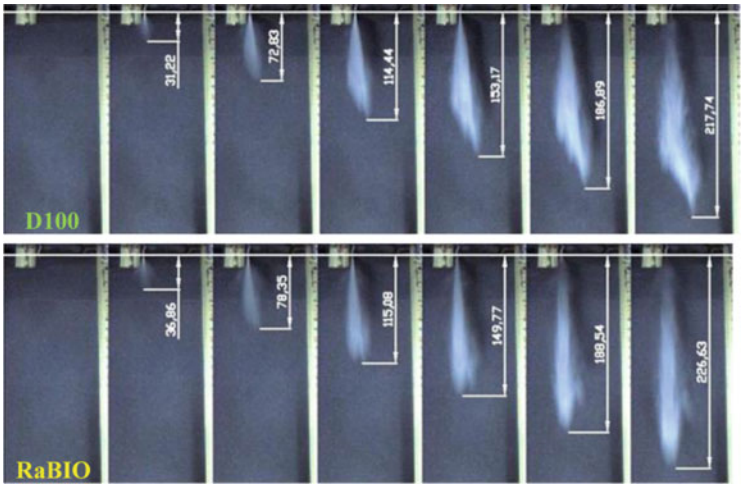

Fig. 6.3 Influence of fuel properties on spray penetration at full load

Table 6.4 Investigation data (Wang et al. 2011)

Injection system/injector	Common rail injector
Nozzle type	Single hole
Nozzle hole diameter	0.16 mm
Injection pressure	1,000, 2,000, 3,000 bar
Injection duration	1.5 ms
Ambient pressure	Up to 40 bar
Ambient temperature	885 K

ensure injection pressures of 1,000, 2,000, and 3,000 bar. The spray chamber with adjustable pressure was filled with nitrogen (ambient) gas. The ambient temperature was fixed at 295 K. The tested ambient densities, controlled by the pressure, were 15 and 30 kg/m^3.

The liquid lengths of D100, PaBIO, and WcBIO are shown in Fig. 6.4. It is evident that biodiesel fuels exhibit longer liquid lengths than mineral diesel. The highest penetration is obtained with PaBIO. Furthermore, the differences of liquid lengths increase as the injection pressure rises.

In Gao et al. (2009) fuel spray tip penetration of *jatropha biodiesel* (JaBIO), WcBIO, and PaBIO was investigated by using a high-speed camera. A

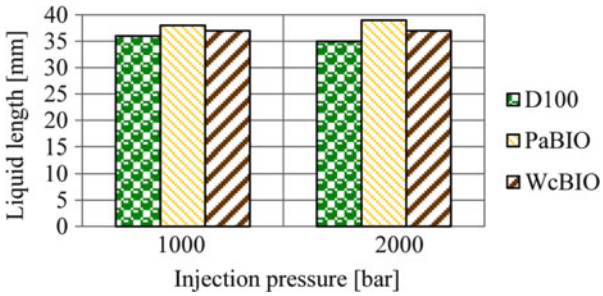

Fig. 6.4 Influence of various fuels on liquid lengths of the spray at various injection pressures

Table 6.5 Investigation data (Gao et al. 2009)

Injection system/injector	In-line mechanically controlled injection system
Nozzle type	Single hole
Length of nozzle hole	0.8 mm
Nozzle hole diameter	0.18 mm
Injection pressure—maximal	430 bar
Injection duration	1.6 ms

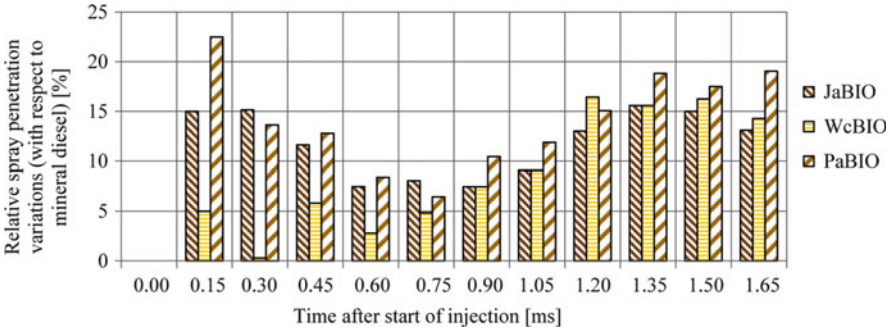

Fig. 6.5 Influence of various fuels on spray penetration history

mechanically controlled fuel injection system with a single-hole injector was used to inject the fuel into a constant volume chamber (Table 6.5).

Among all tested fuels, PaBIO has the highest viscosity. It is known that the increase in fuel viscosity retards the breakup of the spray jet, which results in larger spray droplets. This reduces the total resistance or drag. For this reason, the spray penetration of PaBIO is the highest practically during the whole injection period. Figure 6.5 shows the relative variations of penetration lengths, obtained when D100 was replaced by the tested biodiesels. Interestingly, these variations are the smallest in the period of 0.6–0.8 ms after the start of injection. Before and after this period, the variations are larger.

According to the investigations done so far, one can say that at the same injection pressure, fuelling, injection velocity, and engine operation regime, the spray evolutions of mineral diesel and biodiesels show similar trends. However, because of poorer atomization of biodiesel droplets, biodiesels typically exhibit a slightly higher spray tip penetration than mineral diesel. Furthermore, compared to mineral diesel, biodiesel droplets have a higher ratio of momentum to drag force. This also contributes to longer spray tip penetration of biodiesels (Yoon et al. 2009).

6.1.2 *Influence of Engine Operating Regime*

A change of the engine operating regime is typically accompanied by a change of the injection pressure. This also affects spray penetration lengths and this influence may depend on biodiesel type (Agarwal and Chaudhury 2012; Kegl 2008; Som et al. 2010).

In general, higher engine loads and speeds are accompanied by higher injection pressures which result in higher penetration lengths. But this influence may vary in dependence on the actual operating regime. For example, even at low load (but high engine speed) the biodiesel spray tip penetration may be prolonged up to 15 % with respect to that of mineral diesel.

Ambient pressure and temperature represent two parameters that are not directly related to the engine operating regime. Nevertheless, they influence significantly fuel spray development and it may be of benefit to consider them in the context of engine operating regimes. In general, spray tip penetration and spray width increase as the ambient temperature rises at constant pressure. This is because higher temperature decreases the density of the ambient gas. On the other hand, by keeping the temperature constant and lowering the ambient pressure, the evaporation of the fuel is improved and a decrease of spray tip penetration can be observed.

In Agarwal and Chaudhury (2012) the influence of *engine loads* on the spray penetration of *karanja biodiesel* (KaBIO) and D100 was investigated. A simple mechanically controlled fuel pump with a fuel delivery pressure set at 200 bar and a mechanical injector were used (Table 6.6). The fuel was injected into a customized constant volume spray visualization chamber at various chamber pressures, which simulated various engine loads.

The results show that the spray tip penetration decreases as the chamber pressure increases for both tested fuels. Higher pressure means higher air density in the chamber. This increases the drag force on the droplets at the spray tip. KaBIO exhibited higher penetration lengths at all tested engine loads (Fig. 6.6). This is because the density and viscosity of KaBIO are higher than those of D100 and D100 atomizes more rapidly than KaBIO.

In Som et al. (2010) the influence of injection pressure on spray penetration history was investigated numerically for SoBIO and D100. A common rail injection system was utilized (Table 6.7).

Table 6.6 Investigation data (Agarwal and Chaudhury 2012)

Injection system/injector	In-line mechanically controlled injection system
Nozzle type	Three-nozzle hole
Nozzle hole diameter	0.29 mm
Injection pressure	200 bar

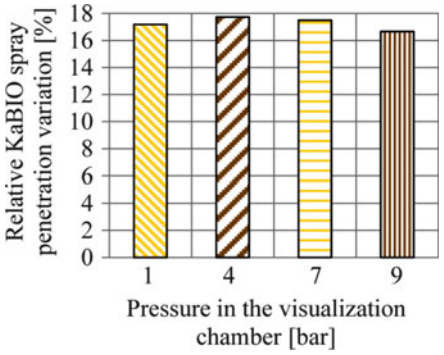

Fig. 6.6 Influence of the ambient pressure on spray penetration of KaBIO with respect to D100

Table 6.7 Investigation data (Som et al. 2010)

Injection system/injector	Common rail injector Detroit diesel
Nozzle type	Mini-sac nozzle with six cylindrical holes
Nozzle hole diameter	0.169 mm
Injection pressure	1,100 bar and 1,300 bar
Injection duration	3 ms
Ambient density	34 kg/m^3
Ambient temperature	300 K

From the results it follows that higher injection pressure yields higher penetration lengths. The relative penetration variation of SoBIO is higher than that of D100 (Fig. 6.7).

In Pogorevc et al. (2008) spray development of RaBIO was investigated at various engine operating regimes (Table 6.3). The effect of pump speed variation at full load is shown in Fig. 6.8. It is evident that lower engine speeds result in a notably shorter spray tip penetrations.

Similar trends were observed at other engine loads. Figure 6.9 illustrates the effect of variable pump speed at partial load (PL) of 50 %.

The obtained experimental results are summarized in Fig. 6.10. It can be seen that engine load influences the spray tip penetration less than engine speed. This can be observed for both fuels, RaBIO and D100.

In Chen et al. (2013) the influence of *injection pressure* on spray tip penetration of WcBIO and D100 was investigated experimentally. The fuels were stored at room temperature of 25 °C and injected into air at ambient temperature and pressure by using a common rail injector with a single hole nozzle (Table 6.8).

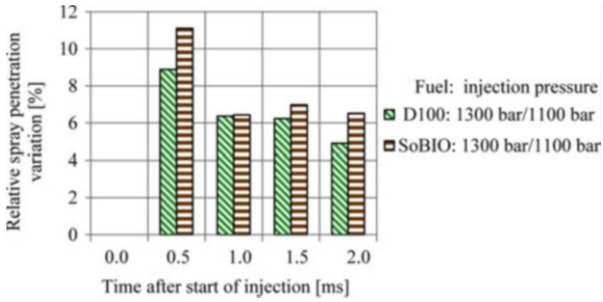

Fig. 6.7 Influence of injection pressure on spray penetration of SoBIO and D100

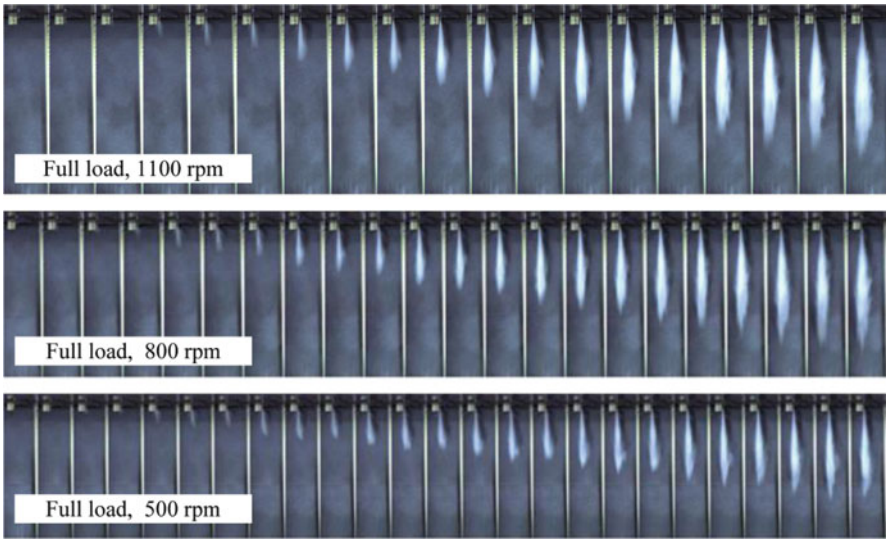

Fig. 6.8 Influence of engine pump speed on RaBIO spray penetration at full load

Figure 6.11 illustrates the obtained spray tip penetration histories. It is evident that tip penetrations of WcBIO and D100 fuels increase with higher injection pressure. This trend can be easily observed by looking at D100 penetration under 300 bar. At 1.5 ms after injection start, the spray tip penetration is 100 mm compared with 140 mm under 1,000 bar. It is interesting that WcBIO shows significantly longer penetrations than D100 at low injection pressures (e.g., 300 bar), but this difference diminishes at higher injection pressures. By regarding the history of the spray development, one can also see that WcBIO penetrates faster than D100 in the early stage of injection. In the later stage D100 catches up and the difference between WcBIO and D100 reduces gradually.

In Park et al. (2009a) the influence of *fuel temperatures* and *ambient gas conditions* on SoBIO spray penetration was investigated by using a common rail injection system (Table 6.9).

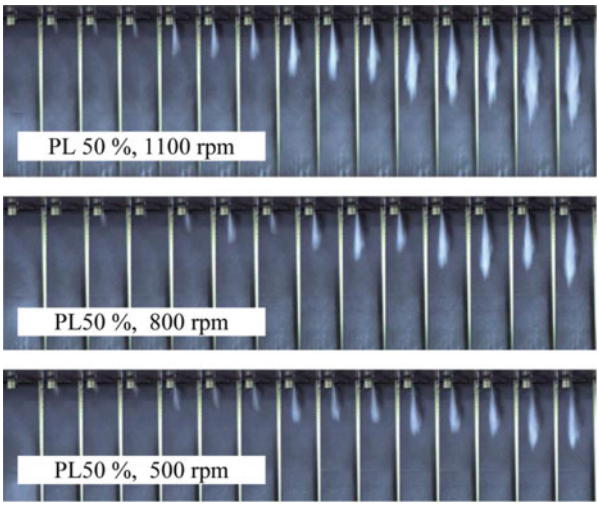

Fig. 6.9 Influence of engine pump speed on RaBIO spray penetration at PL 50 %

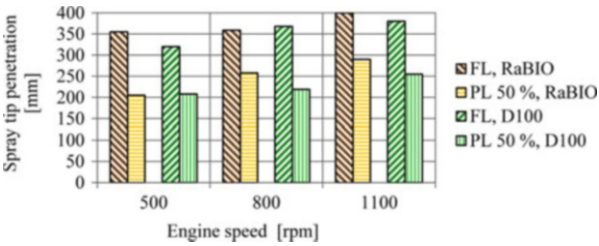

Fig. 6.10 Influence of various engine regimes on RaBIO and D100 spray penetration

Table 6.8 Investigation data (Chen et al. 2013)

Injection system/injector	Common rail injector
Nozzle type	Single hole
Nozzle hole diameter	0.140 mm
Injection pressure—maximum	1,350 bar

The experimentally and numerically obtained results show that the spray tip penetration increases with the increase of the *injection pressure*, which leads to an increase of the initial spray momentum. Furthermore, the spray tip penetration is only slightly affected by the variation of the *fuel temperature*, which causes a variation of fuel properties. On the other hand, increased *ambient air temperature* results in higher spray liquid tip penetration. This is because the ambient air density decreases with rising ambient air temperature. The influence of fuel temperature T_{fuel} and ambient temperature T_{amb} on SoBIO spray penetration under 1,200 bar injection pressure and 20 bar of ambient gas pressure is shown in Fig. 6.12.

In Lee et al. (2005) the SoBIO blend with D100 was tested under various engine regimes, simulated by various injection pressures. The 20 % blend B20 was injected into atmospheric ambient conditions by a common rail injection system (Table 6.10).

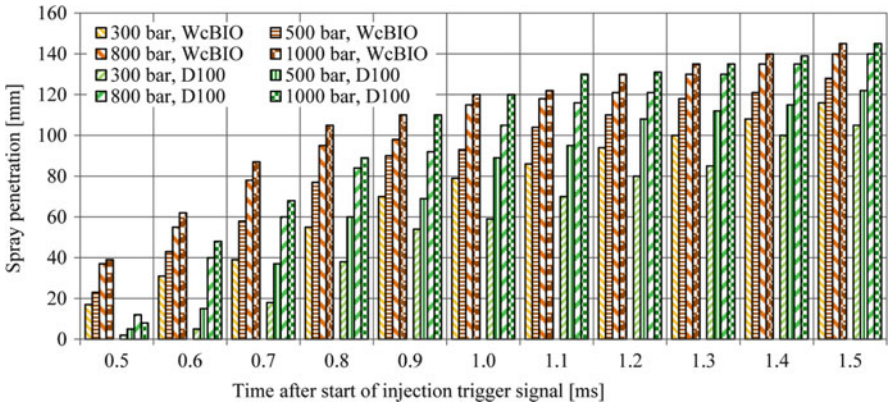

Fig. 6.11 Effect of injection pressure on fuel spray penetration history

Table 6.9 Investigation data (Park et al. 2009a)

Injection system/injector	Common rail injector
Nozzle type	Six cylindrical holes
Length of nozzle hole	0.8 mm
Nozzle hole diameter	0.126 mm
Injection pressure	600 bar and 1,200 bar
Energizing duration	1 ms
Ambient pressure	20 bar

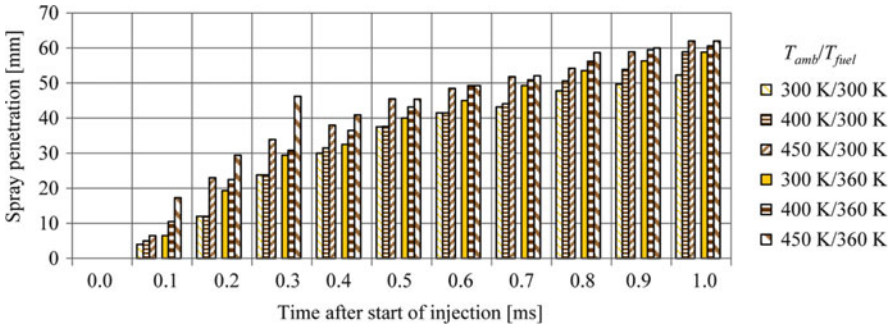

Fig. 6.12 Influence of fuel and ambient air temperature on SoBIO spray penetration history

Table 6.10 Investigation data (Lee et al. 2005)

Injection system/injector	Common rail injector
Nozzle type	Single hole
Nozzle hole diameter	0.3 mm
Injection pressure	400, 600, and 800 bar
Energizing duration	1.0 ms
Ambient pressure	1 bar
Ambient temperature	295 K

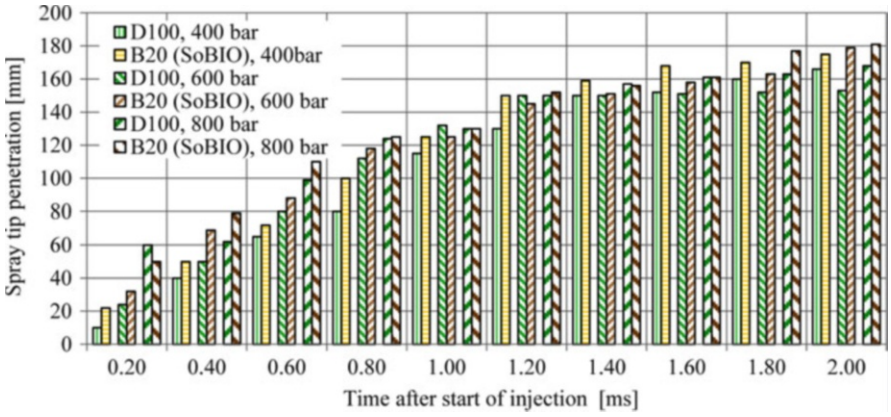

Fig. 6.13 Influence of injection pressure on spray tip penetration history

In Fig. 6.13 the spray tip penetration history of the B20 blend is compared to that of D100 at various injection pressures. Obviously, the spray tip penetration increases at higher injection pressures because of injection velocity rise. It should be noted, however, that the differences between B20 and D100 are rather small.

6.2 Spray Angle

Similarly as spray penetration, the spray angle also depends on biodiesel properties and instantaneous engine operating regime. This influence, however, is also affected by the injector nozzle type.

Battistoni and Grimaldi (2012), Desantes et al. (2009), and Payri et al. (2011) investigated the influence of geometrical parameters of the nozzle on spray development. It was found out that by increasing the nozzle hole diameter or by reducing the length-to-diameter ratio of the hole slightly, the spray angle increases. The shape of the nozzle hole is also important. For example, a conical orifice exhibits low cavitation and turbulence levels inside the orifice. This slows down the primary breakup process and leads to smaller cone angles.

In Battistoni and Grimaldi (2012) the influence of various *nozzle hole types* on D100 and SoBIO spray angle was analyzed. For this purpose, numerical simulation of unsteady multiphase flow inside the injector was employed by using the Eulerian–Eulerian approach. The spray was computed by using the discrete droplet model in the Lagrangian framework. The results show that D100 and SoBIO produce similar cone angles when using a cavitating *cylindrical nozzle hole with sharp edges*. On the other hand, D100 spray angle was significantly smaller than that of SoBIO when a *conical nozzle hole with rounded edges* was used. In this case, SoBIO produces a large cloud after the secondary breakup that increases significantly its global spray cone angle. This result contrasts with the usually observed

trend of narrower angles obtained with biodiesels. Maybe this can be partially attributed to possible inaccuracy of the numerical models, but it surely demonstrates the strong influence of the orifice shape on the spray. Another interesting result was that D100 appeared to be much more sensitive to the orifice shape since it showed very different breakup characteristics: with the rounded conical hole, D100 produced a faster and denser spray which remained compact for a long time. On the other hand, the cylindrical and highly cavitating hole enhanced the D100 spray breakup significantly.

6.2.1 *Influence of Biodiesel Properties*

The fuel spray angle is most significantly influenced by the following properties: *density, viscosity*, and *surface tension* (Kegl 2008; Pandey et al. 2012; Pogorevc et al. 2008; Park et al. 2010; Som et al. 2010; Yoon et al. 2009). In general, biodiesels exhibit higher values of these properties than mineral diesel. Consequently, biodiesels usually form a narrower spray under most operating regimes. Usually, this is also true for the biodiesel blends with mineral diesel (Desantes et al. 2009).

In Wang et al. (2011, 2010) the influence of fuels properties on the spray angle was investigated experimentally under simulated diesel engine conditions (Table 6.4). The results show that by using either PaBIO or WcBIO the spray angles were always smaller than in the case of D100 (Fig. 6.14). One can also see that the differences between both biodiesels decrease as the injection pressure increases.

In Pogorevc et al. (2008) the fuel spray angle was investigated numerically and experimentally (Table 6.3). Numerical simulation was performed by using the AVL Fire program and the Euler–Lagrangian approach. To calculate the *primary breakup* of the spray, the *diesel core injection model* was chosen, while the *secondary breakup* was simulated by using the *wave model*.

Figure 6.15 shows a comparison of the filmed and simulated spray development at pump rotational speed of 500 rpm and full load for D100 and RaBIO. It can be seen that the RaBIO spray is narrower than the D100 spray due to higher spray velocities as a result of higher injection pressure, which is caused by higher viscosity and density of biodiesel.

In Gao et al. (2009) the fuel spray angles of JaBIO, WcBIO, and PaBIO were investigated and compared to that of mineral diesel (Table 6.5). For mechanically controlled injection systems, the spray cone angle history usually shows a gradual increase of the angle during the early phase of injection. This is mainly because the accompanying increase of the injection pressure causes the spray to spread around more intensively, leading to a gradual increase in the cone angle. In the later phase of injection, the cone angle begins to decrease and then stabilizes at a certain value, which depends on the fuel. Namely, in the later phase the outer spray droplets become smaller and diffuse easily, which leads to a reduction of the spray angle.

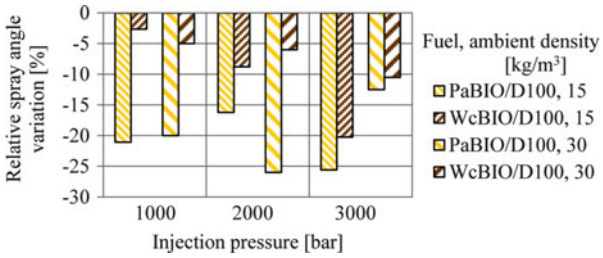

Fig. 6.14 Influence of injection pressure and ambient density on spray angle of PaBIO and WcBIO with respect to D100

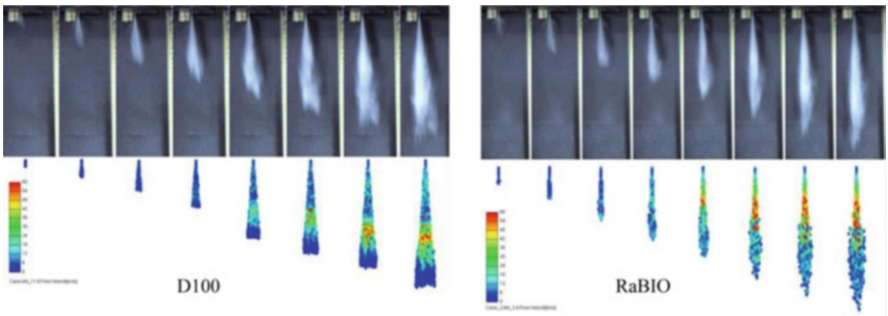

Fig. 6.15 Filmed and simulated spray development at full load

From Fig. 6.16, which shows the relative spray angle variations with respect to D100, one can see that among all tested fuels this behavior is the most exposed for JaBIO. Furthermore, one can see that the stabilized spray angles of all tested biodiesels are lower than that of mineral diesel. The lowest angle is obtained with PaBIO, which has the highest viscosity.

In Valentino et al. (2011) the cone angles of RaBIO and SoBIO blends with D100 were investigated experimentally. The tests were performed on a turbo-charged, water-cooled, 4-valve DI diesel engine, equipped with a common rail injection system (Table 6.11). The results show clearly the dependency of the spray angle on fuel viscosity and ambient gas density.

The spray cone angles are measured at 500 ms after the start of injection. The tested fuels are D100 and its 50 % blends with SoBIO (B50, SoBIO) and with RaBIO (B50, RaBIO). The measurements were carried out on the main injection and averaged over seven sprays and ten shots. The spray cone angle for each tested fuel increased by raising the ambient density. The highest spray cone angles were obtained with D100 which exhibits a viscosity of 3.20 mm^2/s. Somewhat lower angles were observed with SoBIO B50 with 3.46 mm^2/s. RaBIO B50 with the largest viscosity of 3.67 mm^2/s yielded the smallest spray cone angles. Figure 6.17 illustrates nicely the dependence of the spray cone angle on fuel viscosity. One can be seen that lower viscosities result in higher cone angles at any operating condition.

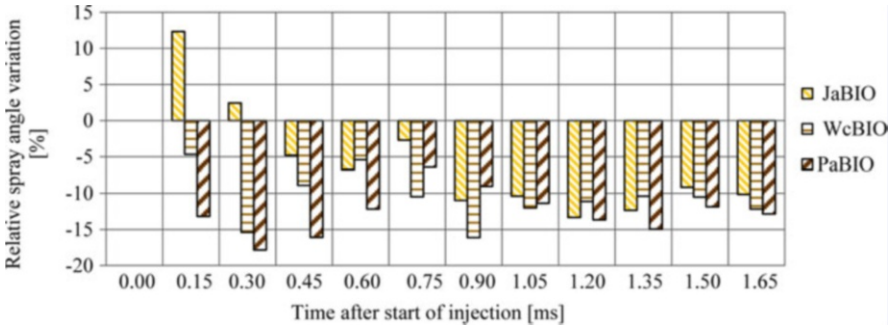

Fig. 6.16 Influence of various biodiesel fuels on spray angle

Table 6.11 Investigation data (Valentino et al. 2011)

Injection model	Bosch CRI 2.2 MW
Nozzle type	Mini-sac seven holes
Nozzle hole diameter	0.136 mm
Injection pressure—maximum	1,600 bar

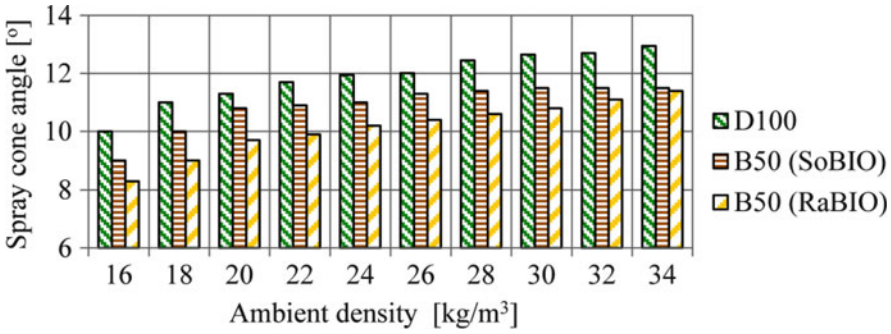

Fig. 6.17 Influence of ambient density on spray cone angle for various fuels

6.2.2 Influence of Engine Operating Regime

A change of the engine operating regime is typically accompanied by a change of the injection pressure. This may also affect the spray angle, depending also on the fuel type (Payri et al. 2011). Lower injection pressures may produce a considerably smaller spray angles than higher pressures. This may be mostly related to the flow regime inside the injection orifice, since at lower injection pressure the flow regime may be closer to a laminar one with low turbulence. On the other hand, high injection pressures increase the turbulence inside the orifice and may cause extensive cavitation. When the fuel exits the nozzle, the radial turbulence velocities eject some fuel away from the main stream and thus promote atomization.

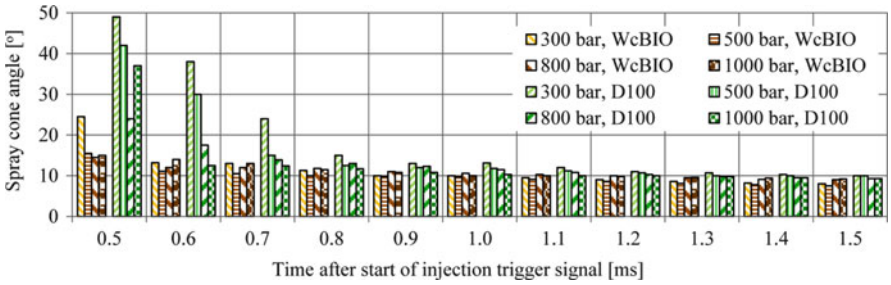

Fig. 6.18 Influence of injection pressure on spray cone angle history

Besides the injection pressure, the ambient pressure and temperature may play an important role. Unfortunately, the spray dependency on these quantities is quite sophisticated. In the literature one can find experimental results (high injection pressure, cylindrical orifice) indicating that high ambient temperature (lower ambient gas density) increases the spray angle. On the other hand, for example, the experimental results on non-cavitating (conical) nozzle holes with rounded edges clearly show that the spray angle increases at higher pressures (higher ambient gas densities) (Payri et al. 2011).

In Chen et al. (2013) spray angles of mineral diesel and WcBIO at various injection pressures were investigated experimentally. The fuels were injected into air at ambient temperature and pressure by using a common rail injector (Table 6.8). Figure 6.18 illustrates the spray cone angle results under *various injection pressures* in dependence on the time after the start of injection. As the spray penetrates, the droplets on the boundaries become smaller and diffuse easily, generating a decreasing trend of spray cone angle. The spray cone angles decrease rapidly after injection start and stabilize at about 10° for each injection pressure. The rate of this decrease, however, varies in dependence on the used fuel. As can be seen from Fig. 6.18, the spray cone angles of both fuels converge to a constant value (steady state of the spray) at around 0.8 ms after the start of injection at 300 bar injection pressure. The steady state is achieved sooner, if the injection pressure increases, for example, at 0.7 ms for 500 and 800 bar. These results show that the differences between various fuels diminish after achieving the steady state. The smaller cone angle of biodiesel after the injection start can probably be mostly attributed to higher *viscosity* of WcBIO, compared to D100.

In Agarwal and Chaudhury (2012) the influence of *engine loads* on the spray cone angle of D100 and KaBIO was investigated by using a simple mechanical control fuel pump and an injector (Table 6.6). The spray cone angle increased as the pressure in the chamber increased. This was observed for all test fuels. At low loads (e.g., at 1 bar of ambient pressure) the ambient air density is lower which results in lower spray cone angles. As the engine load increases (the pressure in chamber increases) the shear resistance exerted by ambient air rises which leads to an increase of the spray angle. The spray cone angle is 10.7° at 1 bar and 16° at 9 bar. Under identical experimental conditions, the spray cone angle of KaBIO is

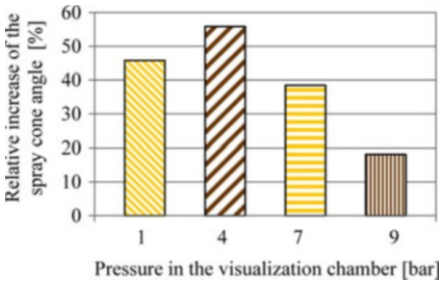

Fig. 6.19 Relative increase of the spray cone angle of KaBIO with respect to D100 under various ambient pressures

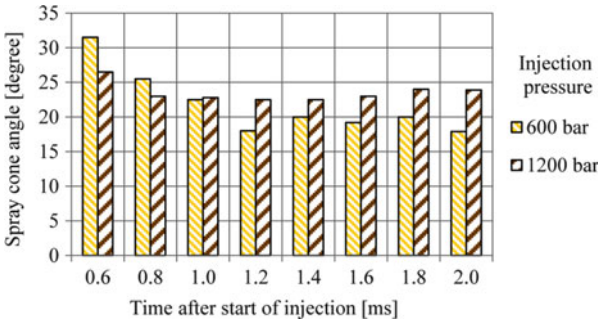

Fig. 6.20 Influence of injection pressure on SoBIO spray cone angle history

higher than that of D100 at all pressure conditions because of different fuel densities (Fig. 6.19).

In Park et al. (2011) the influence of injection pressure on spray angle of SoBIO in a naturally aspirated DI diesel engine with a common rail injection system was investigated. The fuel was injected through a nozzle with six holes with a diameter of 0.128 mm at ambient pressure of 30 bar. At 600 bar of injection pressure, the spray cone angle decreased sharply at the early stage of injection and became stable about 1.2 ms after the start of injection (Fig. 6.20). On the other hand, at 1,200 bar of injection pressure, the variation of the spray cone angle was rather minor.

For a bus diesel MAN engine with a mechanically controlled M fuel injection system (Table 6.3), the experimentally obtained comparison of spray cone angle at various engine speeds at full load is given in Fig. 6.21. It can be seen that the spray cone angles of D100 are higher than those of RaBIO at all engine speeds. For both tested fuels the smallest spray cone angles were observed at 800 rpm (near the peak torque condition).

6.3 Sauter Mean Diameter

The Sauter mean diameter (SMD) of the spray is closely related to the combustion process and consequently to all engine characteristics. Its value influences significantly noise and exhaust emissions, fuel consumption, and engine performance

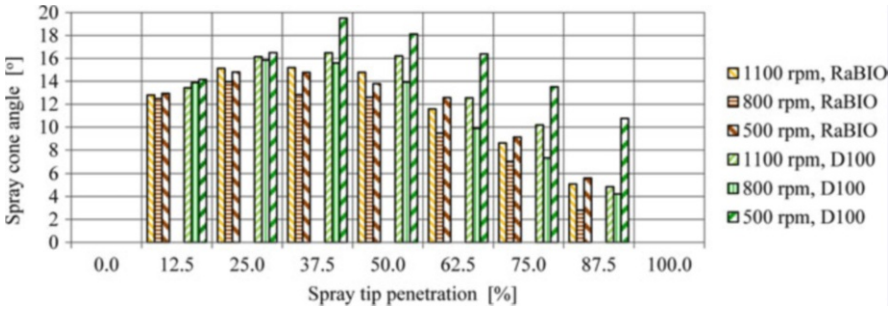

Fig. 6.21 Influence of engine regimes on spray cone angle history

(Battistoni and Grimaldi 2012; Erazo et al. 2010; Park et al. 2008; Shervani-Tabar et al. 2012).

The SMD is a direct indicator of the fuel atomization process. This means that injection pressure, nozzle hole geometry, fuel properties, and ambient conditions will influence its value. For example, when using a cylindrical nozzle hole, the presence of cavitation phenomena depends strongly on the shape of the inlet edge. By rounding the inlet edge, cavitation can be significantly reduced. Since cavitation in the orifice affects spray atomization, this means that a variation of the radius of the inlet orifice will also have a notable impact on the SMD.

6.3.1 Influence of Biodiesel Properties

Fuel atomization and combustion characteristics depend on the following fuel properties: viscosity, surface tension, density, latent heat of vaporization, thermal conductivity, specific heat capacity, boiling point, and heat of combustion. However, *viscosity* and *surface tension* are those that influence fuel atomization and SMD the most (Choi and Oh 2012; Desantes et al. 2009; Pandey et al. 2012; Park et al. 2009b; Wang et al. 2010, 2011).

In general, as the viscosity of the fuel increases, the diameters of fuel droplets increase also. Biodiesels have roughly about 50 % higher viscosity than mineral diesel, which means that larger droplets will form in the spray. The operation of the fuel injector may become less accurate and more deposit formation might be observed on the injector or in the combustion chamber. Higher surface tension also makes the spray harder to break up into smaller droplets. Since surface tension of biodiesels in general is higher than that of mineral diesel, this is another factor promoting larger Sauter mean diameters of biodiesels.

In a fuel spray, the SMD varies along the central axis of the spray and with the radial distance from the axis (Erazo et al. 2010). Experiments with *canola biodiesel* (CaBIO) and D100 revealed that the droplet size may increase with increasing radial distance at all axial locations. This was due to the swirl imparted by the

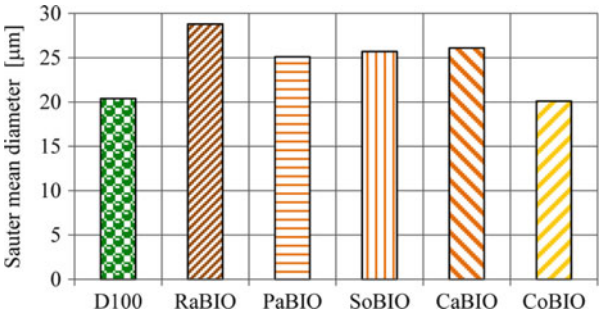

Fig. 6.22 Influence of biodiesel type on SMD

injector, by which the large drops were thrown to the spray edge and took longer to evaporate and burn. The result was an increase of the SMD at the outer edge of the spray. The droplet SMD of CaBIO was smaller than that of D100 at the nozzle exit, implying faster vaporization rates for CaBIO. Furthermore, the droplet sizes in D100 and CaBIO sprays were comparable in the near-injector region and further downstream of the injector. At an axial distance of 30 mm from the injector, however, the SMD of CaBIO was larger than that of the D100 spray. This might be due to the smaller drops of CaBIO evaporating faster than the D100 drops, leaving only the larger drops to remain at this axial location.

In Battistoni and Grimaldi (2012) the influence of various types of nozzle holes on SMD, by using D100 and SoBIO, was investigated by numerical simulation (Table 6.2). The numerical results for the SMD show that SoBIO produces quite larger droplet diameters and its breakup process is slower than that of D100. The main reasons stated are the lower velocities and the lower Weber numbers of SoBIO. The orifice shape had a negligible effect on the SMD, meaning that under given circumstances only the fuel properties determine the average stable non-evaporating droplet size.

A comparison of the SMDs, obtained on a direct fuel injection system for D100, RaBIO, PaBIO, SoBIO, CaBIO, and *coconut biodiesel* (CoBIO) at 80 °C, is given in Fig. 6.22 (Ejim et al. 2007). RaBIO has the largest SMD, which differs more than 40 % from that of D100. CoBIO has the smallest SMD, which is very close to that of D100.

The influence of fuel properties on the SMD was also investigated by (Wang et al. 2010, 2011). The experiments were performed under simulated diesel engine conditions (Table 6.4). The tested ambient densities were 15 and 30 kg/m^3. At both ambient densities the SMD of PaBIO yielded significantly larger Sauter diameters than WcBIO (Fig. 6.23). The difference between both tested biodiesels was larger at higher injection pressure. Both biodiesels always produced larger diameters than D100.

In Chen et al. (2013) spray properties of various fuels, WcBIO being one of them, were investigated experimentally (Table 6.8). The results showed that the SMD of WcBIO increases with the distance from the injector nozzle tip due to momentum loss. This was observed for axial distances of 6 cm and upwards.

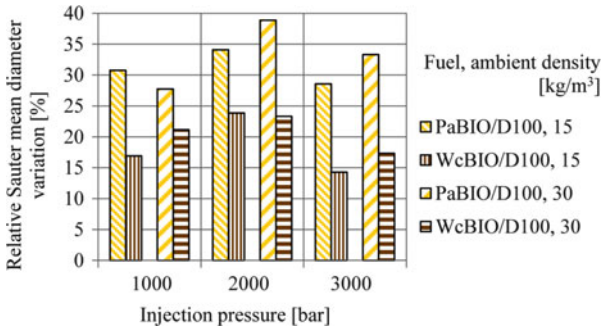

Fig. 6.23 Effect of injection pressure and ambient density on SMD of PaBIO and WcBIO, with respect to D100

Table 6.12 Investigation data (Park et al. 2009b)

Injection system/injector	Common rail injector
Nozzle type	Single hole
Length of nozzle hole	0.80 mm
Nozzle hole diameter	0.30 mm
Injection pressure—maximal	600 bar
Energizing duration	1.2 ms
Ambient temperature	293 K
Ambient pressure	1 bar

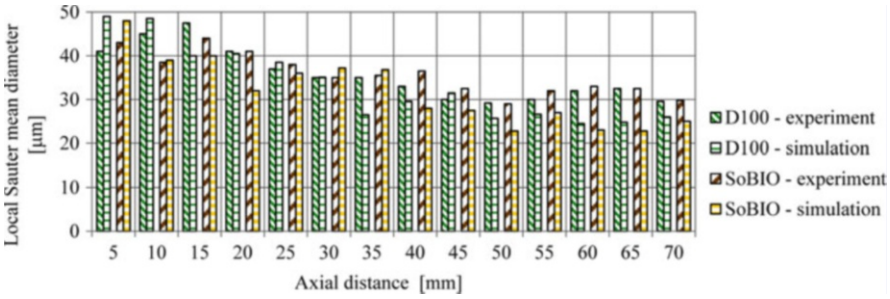

Fig. 6.24 Local SMD history

In Park et al. (2009b) spray atomization characteristics of SoBIO under various ambient pressures were investigated experimentally and numerically. A common rail injector (Table 6.12) was used to inject SoBIO and D100 into a high pressure chamber, filled with nitrogen gas.

The results obtained at 600 bar injection pressure and ambient pressure of 1 bar show that local SMD decreases along the spray axis at the distances from 1 cm up to 5 cm. From 5 cm upwards, it begins to increase slightly. In comparison to D100, the SoBIO exhibited a slightly larger droplet size. However, the difference in SMD between both fuels was relatively small (Fig. 6.24).

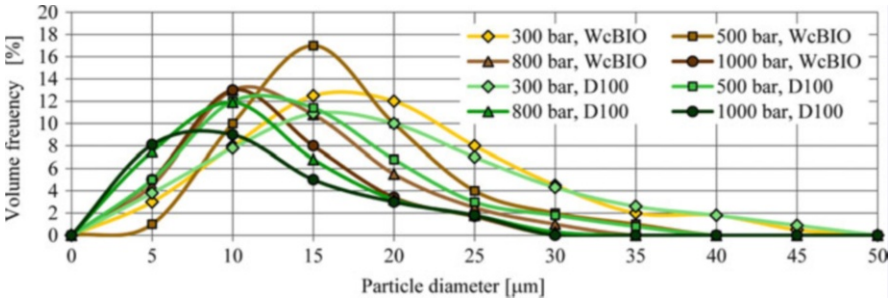

Fig. 6.25 Influence of injection pressure on SMD for various fuels

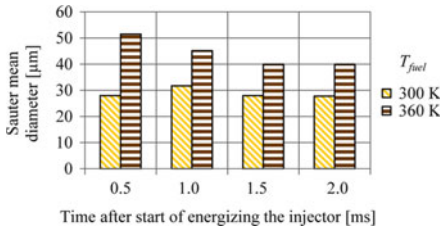

Fig. 6.26 Influence of fuel temperature on SMD history of SoBIO

6.3.2 *Influence of Engine Operating Regime*

A change of the engine operating regime is typically accompanied by a change of the injection pressure, which also affects the SMD. In general, higher injection pressure produces smaller droplets. In this context it may be worth to pay attention also on the fuel temperature, since its variations also influence the SMD.

In Chen et al. (2013) the influence of *variable injection pressure* on the SMD of WcBIO and D100 was investigated experimentally. The fuels at room temperature were injected into air by using a common rail injector (Table 6.8). The injection pressures were 300, 500, 800, and 1,000 bar.

Figure 6.25 illustrates the droplet size distribution (volume frequency) results under *various injection pressures*. All distributions of WcBIO and D100 fuels show a trend towards smaller droplet volumes as the injection pressure increases. D100 consistently exhibits smaller droplet volumes than WcBIO, although at 300 bar the difference is rather small.

In Park et al. (2009a) the effects of *fuel temperature* and *ambient gas temperature* on SoBIO spray atomization behavior were investigated (Table 6.9). It was observed that an increase of fuel temperature results in an increase of overall and local SMD (measured along the spray axis). This is because at higher temperatures small droplets seem to evaporate and vanish very quickly while this process is considerably slower for large droplets. As a result, the SMD increases. The effects of fuel temperature on the overall SMD at ambient temperature of 300 K and ambient pressure of 1 bar are shown in Fig. 6.26. It is evident that the overall

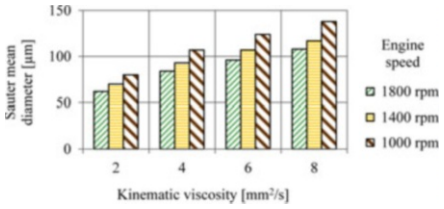

Fig. 6.27 Influence of engine speed and kinematic viscosity on SMD

SMD increases with rising fuel temperature. The measured SMD decreases slightly and stabilizes at some value as the spray develops (Fig. 6.26).

In Tesfa et al. (2010) spray development of RaBIO, WcBIO, *corn biodiesel* (CrBIO), and their blends with D100 was investigated numerically for a turbocharged DI diesel engine. The SMD was determined in dependence on kinematic viscosity for various engine speeds while keeping other engine operating conditions constant. Figure 6.27 shows that when the engine speed increases the SMD decreases. It can also be seen that the SMD increases proportionally with the kinematic viscosity of the fuel.

6.4 Discussion

A replacement of mineral diesel by biodiesel influences the fuel spray development in a rather sophisticated way. This is because this influence depends on many factors, starting from those related to the injection system to those related to biodiesel properties and engine operating conditions. One of the most important parameters of the injection system is the geometry of the injector's nozzle holes. For example, the spray angle may be affected significantly by varying only the rounding radius of the inlet edge of a cylindrical nozzle hole. A reduction of this radius typically increases the turbulences and cavitation inside the orifice, which leads to a wider spray angle. Of course, all such modifications require caution and need to be implemented carefully. For example, too much cavitation may lead to damages of the nozzle.

The task to predict the biodiesel spray development becomes even harder if one takes into account that biodiesels come from a variety of sources and that this variety is also reflected in their properties. A lot of experimental work is therefore needed. In order to reduce the related cost, numerical simulation becomes more and more important. Adequate software, such as AVL Fire or KIVA-3 V, can deliver remarkable results and can be used to reduce experimental work. However, it should be noted that such simulation software typically requires many coefficients of the underlying mathematical models that have to be carefully determined in order to get usable results. This is not an easy task and typically has to be accompanied by experiments.

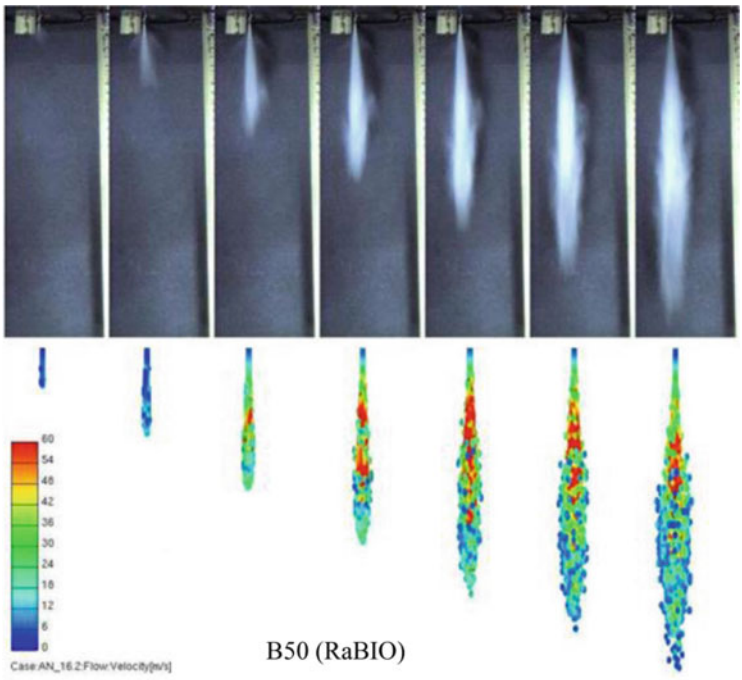

Fig. 6.28 Experimental and simulated spray development at peak torque condition for B50 RaBIO obtained with the approximated primary breakup coefficients

For example, for the primary diesel breakup model (Sect. 2.2.2) the coefficients C_i, $i = 1$, 2, and 3 are needed. One possibility is to build approximation formulas, for example, in the form:

$$C_i = \chi_1^{a_1} \times \chi_2^{a_2} \times \chi_3^{a_3} \ldots \tag{6.1}$$

where a_i are unknown coefficients to be determined and χ_i represents either a fuel physical property, an injection characteristics, or a working regime parameter. The influence of all χ_i parameters on each primary breakup coefficient may be analyzed experimentally and the results may be used to get the coefficients a_i. Under the conditions, given in Pogorevc et al. (2008), the resulting approximations for C_1, C_2, and C_3 are

$$\begin{aligned} C_1 &= \rho_f^{7.808} \times \mu_f^{-2.276} \times \sigma_f^{14.676} \times t_{\text{inj}}^{-31.348} \times s_q^{-9.864} \times n^{-8.391} \\ C_2 &= \rho_f^{-11.507} \times \mu_f^{-0.912} \times \sigma_f^{-23.985} \times q_{\text{inj}}^{38.725} \times p_{\text{ave}}^{15.9889} \times n^{-12.420} \\ C_3 &= \rho_f^{13.447} \times \mu_f^{2.369} \times \sigma_f^{25.764} \times t_{\text{inj}}^{-69.983} \times p_{\text{ave}}^{-23.873} \times n^{-4.015} \end{aligned} \tag{6.2}$$

where ρ_f is fuel density [kg/m^3], μ_f is fuel viscosity [mPas], σ_f is fuel surface tension [N/mm], t_{inj} stands for injection time [ms], p_{ave} is average injection pressure [MPa], $s_q = p_{\text{ave}}/p_{\max}$ is squareness, q_{inj} represents fuelling [mm^3/cycle], and n is pump

speed [min^{-1}]. In some limited context, such approximate models can also be used to get more insight into the influence of some parameters.

For example, in the presented approximate model one can see that fuel *density*, *viscosity*, and *surface tension* appear in the expressions for all three coefficients C_i. If we check the individual terms, however, fuel density and surface tension turn out to be the most influential fuel properties.

Of course, the validity of such approximations has to be verified. The presented approximation model was inserted into the AVL Fire solver steering file and tested on 50 % blend of diesel and rapeseed biodiesel fuel (B50 RaBIO) at engine pump speed of 800 rpm (Pogorevc et al. 2008). The recorded spray development is compared with the simulation results in Fig. 6.28. One can see that good agreement has been obtained with regard to both spray development and its shape (spray angle and penetration).

The comparison given in Fig. 6.28 confirms the correctness of the derived primary breakup coefficient expressions for the used mechanically controlled fuel injection system only, which is a very specific one (nozzle with only one hole of a relatively large diameter). Nevertheless, this example indicates that approximate expressions for various coefficients can be derived in such a way that spray simulations for different fuels and working regimes can be made. In order to get more universal expressions, similar tests would be needed for various injection systems. Their specifications, such as nozzle hole diameter, number of holes, and so on, should of course be included into these expressions.

References

Agarwal, A. K., & Chaudhury, V. H. (2012). Spray characteristics of biodiesel/blends in a high pressure constant volume spray chamber. *Experimental Thermal and Fluid Science, 42*, 212–218.

Battistoni, M., & Grimaldi, N. (2012). Numerical analysis of injector flow and spray characteristics from diesel injectors using fossil and biodiesel fuels. *Applied Energy, 97*, 656–666.

Chen, P. C., Wang, W. C., Roberts, W. L., & Fang, T. (2013). Spray and atomization of diesel fuel and its alternatives from a single-hole injector using a common rail fuel injection system. *Fuel, 103*, 850–861.

Choi, S., & Oh, Y. (2012). The spray characteristics of unrefined biodiesel. *Renewable Energy, 42*, 136–139.

Desantes, J. M., Payri, R., García, A., & Manin, J. (2009). Experimental study of biodiesel blends effects on diesel injection process. *Energy & Fuels, 23*, 3227–3235.

Ejim, C. E., Fleck, B. A., & Amirfazli, A. (2007). Analytical study for atomization of biodiesels and their blends in a typical injector: Surface tension and viscosity effects. *Fuel, 86*, 1534–1544.

Erazo, J. A., Parthasarathy, R., & Gollahalli, S. (2010). Atomization and combustion of canola methyl ester biofuel spray. *Fuel, 89*, 3735–3741.

Gao, Y., Deng, J., Li, C., Dang, F., Liao, Z., Wu, Z., & Li, L. (2009). Experimental study of the spray characteristics of biodiesel based on inedible oil. *Biotechnology Advances, 27*, 616–624.

Kegl, B. (2008). Effects of biodiesel on emissions of a bus diesel engine. *Bioresource Technology, 99*, 863–873.

Kousoulidou, M., Ntziachristos, L., Fontaras, G., Martini, G., Dilara, P., & Samaras, Z. (2012). Impact of biodiesel application at various blending ratios on passenger cars of different fueling technologies. *Fuel, 98*, 88–94.

Kuti, O. A., Zhu, J., Nishida, K., Wang, X., & Huang, Z. (2013). Characterization of spray and combustion processes of biodiesel fuel injected by diesel engine common rail system. *Fuel, 104*, 838–846.

Lee, C. S., Park, S. W., & Kwon, S. I. (2005). An experimental study on the atomization and combustion characteristics of biodiesel blended fuels. *Energy & Fuels, 19*, 2201–2208.

Lin, Y. S., & Lin, H. P. (2011). Spray characteristics of emulsified castor biodiesel on engine emissions and deposit formation. *Renewable Energy, 36*, 3507–3516.

Mancauruso, E., Sequino, L., & Vaglieco, B. (2011). First and second generation biodiesels spray characterization in a diesel engine. *Fuel, 90*, 2870–2883.

Pandey, R. K., Rehman, A., & Sarviya, R. M. (2012). Impact of alternative fuel properties on fuel spray behavior and atomization. *Renewable and Sustainable Energy Reviews, 16*, 1762–1778.

Park, S. H., Kim, H. J., & Lee, C. S. (2010). Fuel spray and exhaust emission characteristics of an undiluted soybean oil methyl ester in a diesel engine. *Energy & Fuels, 24*, 6172–6178.

Park, S. H., Kim, H. J., Suh, H. K., & Lee, C. S. (2009a). Experimental and numerical analysis of spray-atomization characteristics of biodiesel fuel in various fuel and ambient temperatures conditions. *International Journal of Heat and Fluid Flow, 30*, 960–970.

Park, S. H., Kim, H. J., Suh, H. K., & Lee, C. S. (2009b). A study on the fuel injection and atomization characteristics of soybean oil methyl ester (SME). *International Journal of Heat and Fluid Flow, 30*, 108–116.

Park, S. H., Suh, H. K., & Lee, C. S. (2008). Effect of cavitating flow on the flow and fuel atomization characteristics of biodiesel and diesel fuels. *Energy & Fuels, 22*, 605–613.

Park, S. H., Yoon, S. H., & Lee, C. S. (2011). Effects of multiple-injection strategies on overall spray behavior, combustion, and emissions reduction characteristics of biodiesel fuel. *Applied Energy, 88*, 88–98.

Payri, R., Salvador, F. J., Gimeno, J., & Novella, R. (2011). Flow regime effects on non-cavitating injection nozzles over spray behavior. *International Journal of Heat and Fluid Flow, 32*, 273–284.

Pogorevc, P., Kegl, B., & Škerget, L. (2008). Diesel and biodiesel fuel spray simulations. *Energy & Fuels, 22*, 1266–1274.

Shervani-Tabar, M. T., Parsa, S., & Ghorbani, M. (2012). Numerical study on the effect of the cavitation phenomenon on the characteristics of fuel spray. *Mathematical and Computer Modelling, 56*, 105–117.

Som, S., Longman, D. E., Ramírez, A. I., & Aggarwal, S. K. (2010). A comparison of injector flow and spray characteristics of biodiesel with petrodiesel. *Fuel, 89*, 4014–4024.

Tesfa, B., Mishra, R., Gu, F., & Powles, N. (2010). Prediction models for density and viscosity of biodiesel and their effects on fuel supply system in CI engines. *Renewable energy, 35*, 2752–2760.

Valentino, G., Allocca, L., Iannuzzi, S., & Montanaro, A. (2011). Biodiesel/mineral diesel fuel mixtures: Spray evolution and engine performance and emissions characterization. *Energy, 36*, 3924–3932.

Wang, X., Huang, Z., Kuti, O. A., Zhang, W., & Nishida, K. (2010). Experimental and analytical study on biodiesel and diesel spray characteristics under ultra-high injection pressure. *International Journal of Heat and Fluid Flow, 31*, 659–666.

Wang, X., Huang, Z., Kuti, O. A., Zhang, W., & Nishida, K. (2011). An experimental investigation on spray, ignition and combustion characteristics of biodiesels. *Proceedings of the Combustion Institute, 33*, 2071–2077.

Yoon, S. H., Suh, H. K., & Lee, C. S. (2009). Effect of spray and EGR rate on the combustion and emission characteristics of biodiesel fuel in a compression ignition engine. *Energy & Fuels, 23*, 1486–1493.